Evolution of defect densities with height in a HPMC-Si ingot

Rune Søndenå, Halvard Haug, Chang Chuan You, Junjie Zhu, and Marie Syre Wiig

View Online   Export Citation

ARTICLES YOU MAY BE INTERESTED IN

Does LeTID occur in c-Si even without a firing step?
AIP Conference Proceedings **2147**, 140011 (2019); https://doi.org/10.1063/1.5123898

Determination of BO-LID and LeTID related activation energies in Cz-Si and FZ-Si using constant injection conditions
AIP Conference Proceedings **2147**, 140003 (2019); https://doi.org/10.1063/1.5123890

Hydrogen diffusion from PECVD silicon nitride into multicrystalline silicon wafers: Elastic recoil detection analysis (ERDA) measurements and impact on light and elevated temperature induced degradation (LeTID)
AIP Conference Proceedings **2147**, 140009 (2019); https://doi.org/10.1063/1.5123896

Evolution of Defect Densities with Height in a HPMC-Si Ingot

Rune Søndenå [a)] Halvard Haug, Chang Chuan You, Junjie Zhu and
Marie Syre Wiig

Institute for Energy Technology, Instituttveien 18, 2007 Kjeller, Norway

[a)] Corresponding author: rune.sondena@ife.no

Abstract. In this paper we have used a sequential measurement routine to separate and evaluate the effects of two dominant mechanisms for degradation of the carrier lifetime of silicon wafers: Boron-oxygen related light induced degradation (BO-LID) and light and elevated temperature induced degradation (LeTID). Wafers from different heights in a high performance multicrystalline silicon brick have first been illuminated at room temperature to fully activate the BO-LID process in the wafers, followed by an illuminated annealing to activate the more detrimental recombination sites causing LeTID. By isolating the effects of LeTID in this way we hope to improve the analysis and arrive closer to an understanding of the underlying recombination mechanism. The concentration of LeTID defects was observed to increase with height in the bottom half of the ingot and then decrease towards the top in the upper half.

INTRODUCTION

Light and elevated temperature induced degradation (LeTID) has been extensively studied since it was first observed in 2012.[1,2] However, the underlying mechanism is still unknown. LeTID defects are activated during a contact firing step during solar cell production in the presence of a hydrogen-rich anti-reflection coating.[3] Jensen et al. have demonstrated that hydrogen injection activates the LeTID, and not the elevated temperature.[4] Therefore, the involvement of hydrogen, either by itself or in a defect complex, is suspected. Many metallic impurities have been ruled out due to their diffusivity and solubility in silicon. However, a few candidates are still viable candidates; including Co, Cu, and Ni.[5,6] A defect model based on boron-hydrogen pairs has also been proposed.[7]

The study of LeTID in multicrystalline silicon is complicated because of the simultaneous presence of extended crystal defects such as grain boundaries and dislocations. In addition, other recombination active defects, including BO-complexes, metallic impurities and surface recombination may affect the effective lifetime of the wafers. Thus, the effective lifetime can be expressed as a sum of different contributions:

$$\frac{1}{\tau_{effective}} = \frac{1}{\tau_{LeTID}} + \frac{1}{\tau_{BO}} + \frac{1}{\tau_{crystal\ defects}} + \frac{1}{\tau_{other}} + \frac{1}{\tau_{surface}} \tag{1}$$

In this work we assume that the LeTID contribution is the dominating recombination path. However, even if BO-related degradation is more severe in monocrystalline Czochralski silicon, due to the higher content of oxygen, the degradation resulting from boron-oxygen complexes is not negligible in many high performance multicrystalline (HPMC) silicon wafers.[8–10] We also know that the nature of the crystal defects tend to change throughout the height of a HPMC-Si brick, with small grains and a high grain boundary density near the bottom of the ingot, and larger grains, but also larger dislocation clusters towards the top of the ingot. Phosphorus diffusion gettering can typically remove more than 90 % of the interstitial iron in a silicon wafer.[11] We assume that the contribution from other lifetime limiting defects, such as iron, therefore is minimal in gettered wafers. Hydrogen rich dielectric layers can passivate the surfaces reducing the surface recombination considerably. Thus, the τ_{LeTID}, τ_{BO}, and $\tau_{crystal\ defects}$ are the terms

most likely to affect the measured lifetime in phosphorus diffusion gettered and well surface passivated wafers. Most of the early studies on the LeTID evaluated the total degradation in wafers or cells.[12–17] LeTID is then considered the dominating recombination mechanism, and the only term in Eq. 1 that is changing over time. In recent works the effects of BO-related degradation has been accounted for by an initial light soaking at room temperature (RT) prior to LeTID measurements.[8–10,18,19] An approach where a sequential measurement routine, of first measuring the degradation at RT followed by the degradation during an illuminated annealing, has been proposed to separate the effects of LeTID from the BO-degradation.[20]

In the present work we have measured the degradation in wafers from different heights of a HPMC Si brick using a sequential measurement approach. The total degradation has been decomposed into contributions from BO-degradation and LeTID.

EXPERIMENTAL DETAILS

Boron doped HPMC Si wafers from several different heights in an ingot has been studied with respect to degradation of the minority carrier lifetime. The p-type wafers, with an intentionally low resistivity of approximately 1 Ω-cm, were processed as shown in Fig. 1. Injection dependent minority carrier lifetimes were measured on 5×5 cm^2 pieces of the passivated wafers using the quasi steady-state photoconductance technique (QssPC) on a Sinton lifetime tester WCT-120TS. The lifetime values were measured at approximately 25 °C, and lifetimes are extracted at $\Delta n = 0.1 \times p_0$. An initial dark annealing for 20 minutes at 200 °C was used on all wafers prior to measurements. After the initial annealing step the degradation was measured in two sequences to separate the effects of BO-related degradation from the LeTID. First the BO-degradation was induced by illuminating the samples with low intensity LED light at room temperature. A light intensity of approximately 5 mW/cm^2 for more than 72 hours was used, in an automated measurement process.[21,22] A second and stronger degradation is induced at an elevated temperature using higher intensity LED light of approximately 70 mW/cm^2 while heating the samples to 150 °C on a hotplate. This second degradation has been attributed LeTID.

Damage etch in an HNA-solution (HF, nitric acid, acetic acid)

$POCl_3$ emitter in-diffusion in a tube furnace

PECVD deposition of an SiN_X:H anti-reflection coating

Simulated contact firing without metal pastes present

Emitter etch-back in an HNA-solution (HF, nitric acid, acetic acid)

Surface passivation using an a-Si:H/SiN_X:H stack deposited by PECVD

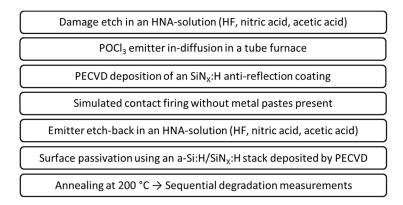Annealing at 200 °C → Sequential degradation measurements

FIGURE 1. The wafers were phosphorus diffusion gettered[11,23] and subjected to a contact firing temperature profile without screen printing of metal contacts.[20] After a 20-minute dark anneal at 200 °C the wafers were subjected to a sequential degradation routine; first illumination at RT, followed by an illuminated annealing. Surface recombination velocities of less than 5 cm/s are expected with this stack passivation.[24]

To quantify and compare degradation in wafers with different initial lifetimes the normalized lifetimes $\tau_{effective}(t)/\tau_0$, and the normalized defect densities (*NDD*) are used. The *NDD* in wafers from different heights are calculated based on the following equation:

$$NDD(t) = \frac{1}{\tau_{effective}(t)} - \frac{1}{\tau_0}.$$ (2)

For both approaches τ_0 represent the starting lifetime value in each measurement sequence while $\tau_{effective}(t)$ is the measured lifetime during the following illumination or illuminated annealing process.
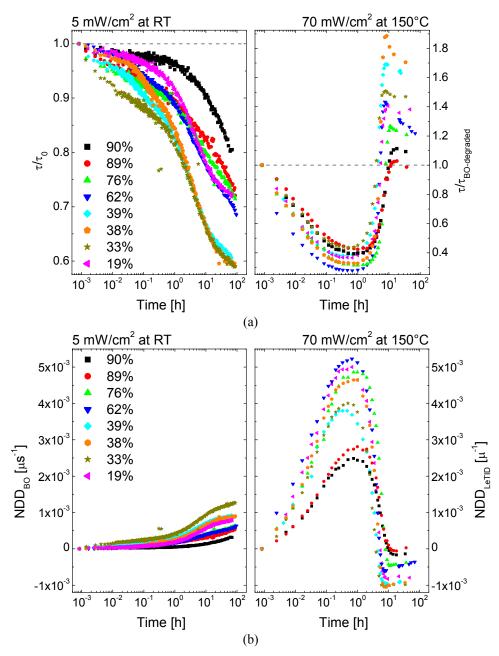
FIGURE 2. Normalized effective lifetimes as a function of time measured using QssPC are shown in a). The corresponding normalized defect densities are shown in b). The first measurement sequence (left) under illumination at RT is attributed BO-related degradation, while the second measurement sequence (right) under illuminated annealing represent the LeTID.

RESULTS AND DISCUSSION

The normalized effective lifetimes and the normalized defect densities in wafers from different heights in a HPMC Si brick throughout the two measurement sequences are shown in Figures 1a and 1b, respectively. Degradation under illumination at room temperature, attributed boron-oxygen complexes, changes considerably with height in the brick. A general trend shows decreasing amounts of BO-related degradation with increasing height in the brick. This corresponds well with the expected exponential reduction of the oxygen concentration with increasing heights in directionally solidified silicon ingots.[25,26] The lowest position, however, deviates from this trend with less BO-degradation than expected. Figure 1a shows that wafers from the bottom part of the brick exhibits signs of both fast

and slow recombination centres, which is characteristic for BO-LID seen in Cz-Si wafers.[21,27] However, the degradation under illumination at RT does not seem to stabilize, even after 72 hours of illumination. This is especially visible in wafers from the upper parts of the brick. A very slow activation of BO-defects with low oxygen levels may explain this. An alternative explanation could be the emerging activation of LeTID defects at temperatures as low as RT. Vargas et al. have recently reported on lifetime effects in p-type Si wafers at RT that may indicate such behaviour.[28]

The normalized defect densities shown in Fig. 1b are calculated according to Eq. 2. LeTID is by far the most recombination active defect when fully activated. After about 40-60 minutes of illuminated annealing the NDD_{LeTID} is about 5 times higher than the maximum NDD_{BO}. Prolonged illuminated annealing leads to recovery of much of the initial lifetime, exceeding the lifetime after BO-degradation at RT. We must therefore conclude that the lifetime recovery is a result of deactivation of both BO-defects and LeTID-defects under comparable conditions and timescales. A secondary degradation seen after illuminated annealing for more than 10 hours has been observed in similar studies and attributed degradation of the hydrogen rich passivation layer.[29,30]
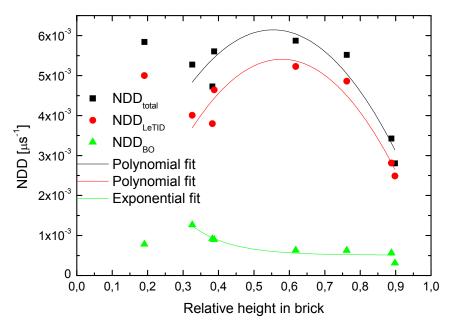

FIGURE 3. Maximum NDD values calculated according to Eq. 2 for the total-, LeTID-, and BO-related degradation, respectively. Second order polynomial fits and exponential fits are generated without the wafer from the lowest position in the bricks.

Figure 3 shows maximum normalized defect densities as a function of height in the ingot, i.e. after 72 hours of illumination at RT for BO-LID, and after approximately 40 minutes of illuminated annealing for LeTID. An exponential fit is used to illustrate the trend in the NDD_{BO}. The NDD_{total} and the NDD_{LeTID} show comparable curves, with increasing defect concentrations with increasing height in the lower parts of the ingot. At about 55-60% of the height there is a turning point, and in the upper half of the ingot the defect densities decrease with increasing height. Polynomial fits are used to indicate this trend. As the LeTID is the dominating recombination mechanism, the effects of adjusting for the BO-degradation are small; A small reduction in the absolute value, and a slight shift of the turning point near the middle of the ingot height. The general trend corresponds well with previous studies of the LeTID as a function of ingot height.[31,32]

The effect of changes in the crystal structure is largely neglected in the current work. We fully expect the crystal structure to change over the height of a brick, potentially affecting the effective lifetime as well as the corresponding defect density. Wafers from lower parts of HPMC Si ingots tend to have smaller grains and a higher density of grain boundaries. Crystal defects will most strongly affect the initial effective lifetime, thus underestimating the BO defect density low in the ingot. Our results show that this may cause deviations from the general trends even as high up as 19% of the ingot height. Growth of dislocation clusters may potentially limit the effective lifetime considerably in the upper parts of the ingots as well. For positions above 62% of the ingot height, saturation of the degradation at RT is not observed. This can either be attributed to incomplete BO-related degradation or onset of LeTiD even at room

temperature. As the NDD_{BO} must be considered small compared to the NDD_{LeTID} small, and the time associated with BO-LID is quite well known from p-type Czochralski silicon[33–35], onset of LeTiD at RT is more likely to explain the observed behaviour. If this is the case the defect concentrations of the LeTID defect might be slightly underestimated for the upper part of the ingot.

SUMMARY

A sequential measurement approach has been used do distinguish between the degradation caused by BO-complexes and the degradation attributed LeTID in wafers from different heights of a HPMC-Si brick. The normalized defect densities of the two light sensitive defects throughout the height of an ingot show that LeTID is by far the dominating defect when fully activated. However, the contribution from BO-complexes is not negligible. The boron-oxygen related degradation corresponds well with the expected decrease in the oxygen levels with increasing height in an ingot. The NDD_{LeTID} shows an increase with height in the lower half of the ingot, while above a turning point at about 55-60% height there is a decrease in the defect concertation attributed LeTID towards the top of the ingot. Potential incomplete activation of the BO-complexes, emerging activation of LeTID under illumination at room temperature, and crystal defects are still elements that may affect the measured lifetimes as well as the estimated defect densities.

ACKNOWLEDGMENTS

REFERENCES

1. K. Ramspeck, S. Zimmermann, H. Nagel, A. Metz, Y. Gassenbauer, B. Birkmann, and A. Seidel, in *27th EUPVSEC* (Frankfurt, Germany, 2012).
2. T. Niewelt, F. Schindler, W. Kwapil, R. Eberle, J. Schön, and M.C. Schubert, Prog. Photovoltaics Res. Appl. **26**, 533 (2018).
3. C. Vargas, K. Kim, G. Coletti, D. Payne, C. Chan, S. Wenham, and Z. Hameiri, IEEE J. Photovoltaics **8**, 413 (2018).
4. M.A. Jensen, A. Zuschlag, S. Wieghold, D. Skorka, A.E. Morishige, G. Hahn, and T. Buonassisi, J. Appl. Phys. **124**, 85701 (2018).
5. D. Bredemeier, D.C. Walter, and J. Schmidt, Sol. Rapid Res. Lett. **2**, 1700159 (2018).
6. M.A. Jensen, A.E. Morishige, S. Chakraborty, R. Sharma, H.S. Laine, B. Lai, V. Rose, A. Youssef, E.E. Looney, S. Wieghold, J.R. Poindexter, J.-P. Correa-Baena, T. Felisca, H. Savin, J.B. Li, and T. Buonassisi, IEEE J. Photovoltaics **8**, 448 (2018).
7. T.H. Fung, M. Kim, D. Chen, C.E. Chan, B.J. Hallam, R. Chen, D.N.R. Payne, A. Ciesla, S.R. Wenham, and M.D. Abbott, Sol. Energy Mater. Sol. Cells **184**, 48 (2018).
8. T. Luka, S. Grosser, C. Hagendorf, K. Ramspeck, and M. Turek, Sol. Energy Mater. Sol. Cells **158**, 43 (2016).
9. T. Luka, M. Turek, C. Kranert, S. Grosser, and C. Hagendorf, Energy Procedia **124**, 759 (2017).
10. M. Kim, D. Chen, M. Abbott, S. Wenham, and B. Hallam, AIP Conf. Proc. **1999**, 130010 (2018).
11. M.S. Wiig, K. Adamczyk, H. Haug, K.E. Ekstrøm, and R. Søndenå, Energy Procedia **92**, 886 (2016).
12. A. Zuschlag, D. Skorka, and G. Hahn, Prog. Photovoltaics **25**, 545 (2017).
13. M.A. Jensen, A. Morishige, J. Hofstetter, and T. Buonassisi, IEEE J. Photovoltaics **7**, 980 (2017).
14. J.M. Fritz, A. Zuschlag, D. Skorka, A. Schmid, and G. Hahn, Energy Procedia **124**, 718 (2017).
15. D. Bredemeier, D. Walter, S. Herlufsen, and J. Schmidt, AIP Adv. **6**, 035119 (2016).
16. H.C. Sio, H. Wang, Q. Wang, C. Sun, W. Chen, H. Jin, and D. Macdonald, Sol. Energy Mater. Sol. Cells **182**, 98 (2018).
17. C. Chan, T.H. Fung, M. Abbott, D. Payne, A. Wenham, B. Hallam, R. Chen, and S. Wenham, Sol. Rapid Res. Lett. **1**, 1600028 (2017).
18. F. Fertig, K. Krauß, and S. Rein, Phys. Status Solidi – Rapid Res. Lett. **9**, 41 (2014).
19. K. Krauß, A.A. Brand, F. Fertig, S. Rein, and J. Nekarda, IEEE J. Photovoltaics **6**, 1427 (2016).

20. R. Søndenå and M.S. Wiig, J. Appl. Phys. **125**, 85701 (2019).
21. T.U. Nærland, H. Haug, H. Angelskår, R. Søndenå, E.S. Marstein, and L. Arnberg, IEEE J. Photovoltaics **3**, 1265 (2013).
22. R. Søndenå and A. Ghaderi, in *29th EUPVSEC* (Amsterdam, Netherlands, 2014).
23. M. Syre, S. Karazhanov, B.R. Olaisen, A. Holt, and B.G. Svensson, J. Appl. Phys. **110**, 24912 (2011).
24. H. Haug, R. Søndenå, M.S. Wiig, and E.S. Marstein, Energy Procedia **124**, 47 (2017).
25. K. Tang, M. Syvertsen, R. Fagerberg, C. Modanese, and M. Di Sabatino, in *CSSC-6* (Aix-Les-Baines, France, 2012).
26. A.-K. Søiland, J.O. Odden, B. Sandberg, K. Friestad, J. Håkedal, E. Enebakk, and S. Braathen, in *CSSC-6* (Aix-Les-Bains, France, 2012).
27. B. Hallam, M. Abbott, T. Nærland, and S. Wenham, Phys. Status Solidi - Rapid Res. Lett. **10**, 520 (2016).
28. C. Vargas, G. Coletti, C. Chan, D. Payne, and Z. Hameiri, Sol. Energy Mater. Sol. Cells **189**, 166 (2019).
29. D. Sperber, A. Graf, D. Skorka, A. Herguth, and G. Hahn, IEEE J. Photovoltaics **7**, 1627 (2017).
30. D. Sperber, A. Heilemann, A. Herguth, and G. Hahn, IEEE J. Photovoltaics **7**, 463 (2017).
31. K. Petter, K. Hübener, F. Kersten, M. Bartzsch, F. Fertig, and J. Müller, in *CSSC-9* (Tempe, Arizona, USA, 2016).
32. F. Kersten, P. Engelhart, H.-C. Ploigt, F. Stenzel, K. Petter, A. Szpeth, M. Bartzsch, A. Stekolnikov, M. Scherff, J. Heitmann, and J.W. Müller, in *31st EUPVSEC* (Hamburg, Germany, 2015).
33. T.U. Nærland, H. Angelskår, and E.S. Marstein, J. Appl. Phys. **113**, 193707 (2013).
34. J. Schmidt and K. Bothe, Phys. Rev. B **69**, 24107 (2004).
35. H. Hashigami, Y. Itakura, and T. Saitoh, J. Appl. Phys. **93**, 4240 (2003).